International Journal of Mass Spectrometry 291 (2010) 73–83

Contents lists available at ScienceDirect

International Journal of Mass Spectrometry

journal homepage: www.elsevier.com/locate/ijms

# Complexation of glycine by manganese (II) in the gas phase: A theoretical study

M. Hassan Khodabandeh[a], Mehdi D. Davari[a], Mansour Zahedi[a,*], Gilles Ohanessian[b,**]

[a] Department of Chemistry, Faculty of Sciences, Shahid Beheshti University, G.C., Evin, 19839-6313 Tehran, Iran
[b] Laboratoire des Mécanismes Réactionnels, Département de Chimie, Ecole Polytechnique, CNRS, 91128 Palaiseau Cedex, France

ARTICLE INFO

*Article history:*
Received 1 October 2009
Received in revised form 17 January 2010
Accepted 19 January 2010
Available online 25 January 2010

*Keywords:*
Glycine
$Mn^{2+}$
Complexation
Gas phase metal ion chemistry
Ab initio calculations

ABSTRACT

The interaction of $Mn^{2+}$, being in three possible spin states, with glycine has been studied using quantum chemical calculations in the gas phase. Seven modes of interaction have been considered in all cases. Investigation of manganese complexes having various possible spin state including high, intermediate and low spins shows that the most stable complexes are high spin (total electron spin $S = 5/2$). Calculations show that the most stable mode of binding involves the simultaneous interaction of $Mn^{2+}$ with two oxygen atoms of the zwitterionic conformers of glycine ($\eta^2$-O,O ($CO_2^-$)), while the second preferred binding site consists of chelation between the carbonyl oxygen and the amino nitrogen ($\eta^2$-O,N). These results indicate that the relative affinity of $Mn^{2+}$ and the glycine zwitterion makes this isomer of glycine more stable than others, even though it is not stable in its isolated form. The results are in accord with those of previous reports for some doubly charged cations and in some cases with monocations. The nature of the interaction between manganese metal cation and glycine is also discussed employing natural population and molecular orbital analyses. It has been found that electrostatics contribution plays a crucial role in this interaction. Complexation energy ($D_0$) of the low lying energy isomer, for the most stable sextet spin state, has been obtained as about 156 kcal/mol. It has also been shown that the computed vibrational frequencies could aid in identification of the most stable $Mn^{2+}$–glycine complex.



## 1. Introduction

It is well recognized that manganese (Mn) ion plays significant roles in many key biological and environmental processes as a constituent of some enzymes and an activator of several other enzymes [1–4]. Manganese proteins, for example, are important in the oxygen evolution catalyzed by the proteins of photosynthetic reaction center and are involved in the metabolism of amino acids and proteins [5]. In addition, manganese as a divalent metal ion plays a significant role in RNA structure and catalysis [6,7]. In many manganese proteins the manganese is in the II oxidation state [4].

Recently, transition metal cationization has proven to be a very useful tool for the elucidation of the primary structure of amino acids [8–10]. The knowledge of the metal cation binding site in the interactions between these metal ions and amino acids is therefore the first step for understanding the mechanism of relevant biological processes [11]. Further, the details of intrinsic properties such as the local interactions that take place between the metal cation and the biomolecule could be understood by the gas phase study of the metal cation–amino acid complexes [12]. These studies are also useful in evaluating the thermochemical data of reaction processes and in developing models of bonding [13]. In addition, such information aids in interpreting the fragmentation mechanisms in mass spectrometry experiments used for the elucidation of the sequence of peptides cationized by various metal cations [14–19].

The interaction of different metal cations with glycine (Gly), the prototype compound of ions with amino acids, have been studied extensively by several authors from experimental and theoretical points of view [13,20–44]. The structure of glycine cationized with singly charged metal cations has been analyzed in previous theoretical works [13,31–44]. It has been found that the lowest isomer of cationized glycine is a charge solvated structure. These calculations led to the result that charge solvation by chelation of cation between nitrogen and the carbonyl oxygen seems to be the most favorable for most of glycine–mono cation complexes. In contrast, extensive studies on gaseous glycine have shown that zwitterions (salt bridge forms) are not even local minima on the potential energy surface of glycine [31,45–52]. One of the ways to induce the natural to zwitterion transition in the gas phase is favoring the zwitterion by attaching a charged species such as an atomic metal cation [13,32,34–37,43,44,53]. Such studies have established that for complexation of glycine by doubly charged cations the salt bridge structure, in which the metal ion interacts with the car-

* Corresponding author. Tel.: +98 21 22401765/29902889; fax: +98 21 22401765/22431663.
** Corresponding author. Tel.: +33 1 69 33 48 01; fax: +33 1 69 33 48 03.
*E-mail addresses:* mansourzahedi@yahoo.com, m-zahedi@cc.sbu.ac.ir (M. Zahedi), gilles.ohanessian@polytechnique.fr (G. Ohanessian).

1387-3806/$ – see front matter © 2010 Elsevier B.V. All rights reserved.
doi:10.1016/j.ijms.2010.01.012

boxylate end of zwitterionic glycine, is preferred in most cases. It has been, in particular, reported that several factors may influence the relative energy of charge solvated and zwitterion isomers [13,34,35,37,39,44].

Despite numerous studies [13,20–44] on gaseous metal cationized glycine, however, to the best of our knowledge, the interaction of manganese and amino acids has not been studied theoretically. The aim of this work is to study the structure of Mn(II) complexes with glycine as a typical amino acid. To obtain a comprehensive understanding of manganese complexation three possible spin states namely high, low and intermediate spin states have been investigated using quantum chemical methods. The examination of gas phase glycine–manganese (Gly–$Mn^{2+}$) complexes provides fundamental information about the probable manganese spin state and glycine coordination sites. Our results show that as in the case of other divalent metal cations [13,34,35,37,39,44], for all three spin multiplicities the ground state structure is the zwitterionic one, $\eta^2$-O,O ($CO_2^-$), mainly due to the large electrostatic interaction between the divalent metal cation and the $CO_2^-$ group. Charge solvated structure by chelation of Mn between nitrogen and carbonyl oxygen ($\eta^2$-N,O) seems to be the second most favorable isomer for Gly–$Mn^{2+}$. These results verify the capability and correspondence of both B3LYP and MP2 among various methods in evaluation of energy of $Mn^{2+}$ amino acid complexes.

## 2. Computational details

The adequacy of density functional methods for study of the conformational behaviors of glycine has been the subject of several papers [54,55]. It is shown that hybrid functionals, in particular the B3LYP [56–58], provide very similar structural parameters compared with second order Moller-Plesset (MP2) [59,60] and the density functional vibrational frequencies and intensities are in good agreement with experimental data. Moreover, the hybrid B3LYP has been shown to provide accurate results for many transition metal-containing systems [61–65]. However, it is always convenient to confirm the reliability of the B3LYP method applied to these kinds of systems by using highly accurate methods. Thus, we have performed geometry optimization and vibrational frequency calculations at the MP2 level, and also single-point energy calculations on some B3LYP geometries using the MP2 and CCSD(T) methods.

Geometry optimization and frequency calculations have been performed using the 6-31G(d,p) [66,67] basis set for all atoms without constraints by applying an unrestricted formalism. Single point calculations have been carried out using the 6-311+G(3df,2p) [66,67] basis set for the O, N, C, and H atoms, and the [14s11p6d3f/8s6p4d1f] Wachters basis set for Mn [68]. This basis is denoted as "basis" for simplicity herein. To eliminate the inconsiderable effect of spin contamination errors in energy estimation all the open shell single point calculations have been carried out using a restricted open shell (RO) formalism. We have performed our single point calibration calculation for complexation of some small molecules with $Mn^{2+}$ using the CCSD(T) method [69] and high level basis set which is indicated by CCSD(T)/basis. Net atomic charges and spin densities were obtained using the natural population analysis of Weinhold et al. [70]. All the calculations were performed by means of the Gaussian 98 program [71].

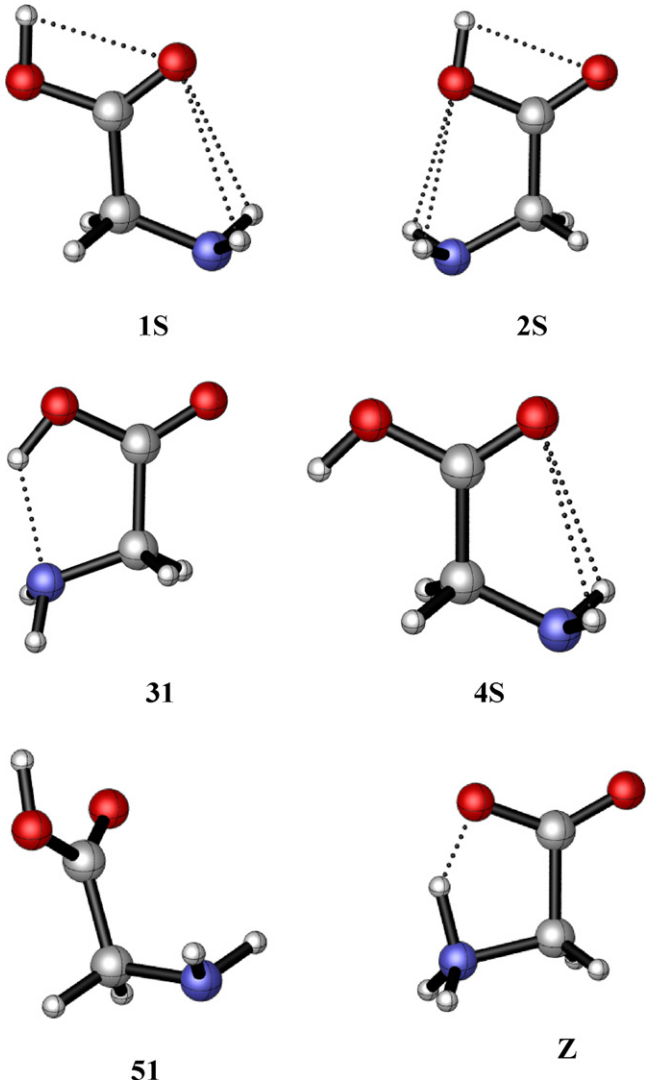


**Fig. 1.** Selected conformations of glycine considered in this study.

## 3. Results and discussion

### 3.1. Glycine conformations

The conformations of glycine have been the subject of many theoretical and experimental studies [31,45–52]. One of the com-

**Table 1**
Relative energies (in kcal/mol) of some of the lowest conformations of glycine at various computational levels.

| Computational level | 1S | 2S | 31 | 4S | Z[a] | Ref. |
|---|---|---|---|---|---|---|
| MP2/6-31G(d)//HF/6-31G(d,p) | 0.0 | 1.7 | 1.5 | 6.5 | – | [46] |
| MP2/6-31G(d)//MP2/6-31G(d) | 0.0 | 1.6 | 1.2 | 6.5 | – | [31] |
| CCSD(T)/DZP//CCSD/DZP | 0.0 | 1.5 | 1.0 | – | – | [47] |
| MP4/6-311++G(d,p)//MP2/6-311++G(d,p) | 0.0 | 1.5 | 0.7 | 5.5 | – | [48] |
| MP2/extended basis//MP2/6-311++G(d,p) | 0.0 | 1.7 | 0.4 | 4.9 | – | [48] |
| B3LYP/DZP//B3LYP/DZP | 0.0 | 1.5 | 0.2 | – | – | [49] |
| B3LYP/6-31G(d,p)//B3LYP/6-31G(d,p) | 0.0 | 1.7 | 0.7 | 5.7 | 17.2 | This work |
| MP2/basis//B3LYP/6-31G(d,p) | 0.0 | 1.6 | 0.5 | 5.0 | 15.7 | This work |

[a] Not a local minimum. Optimized structure has been obtained by imposing constraints.

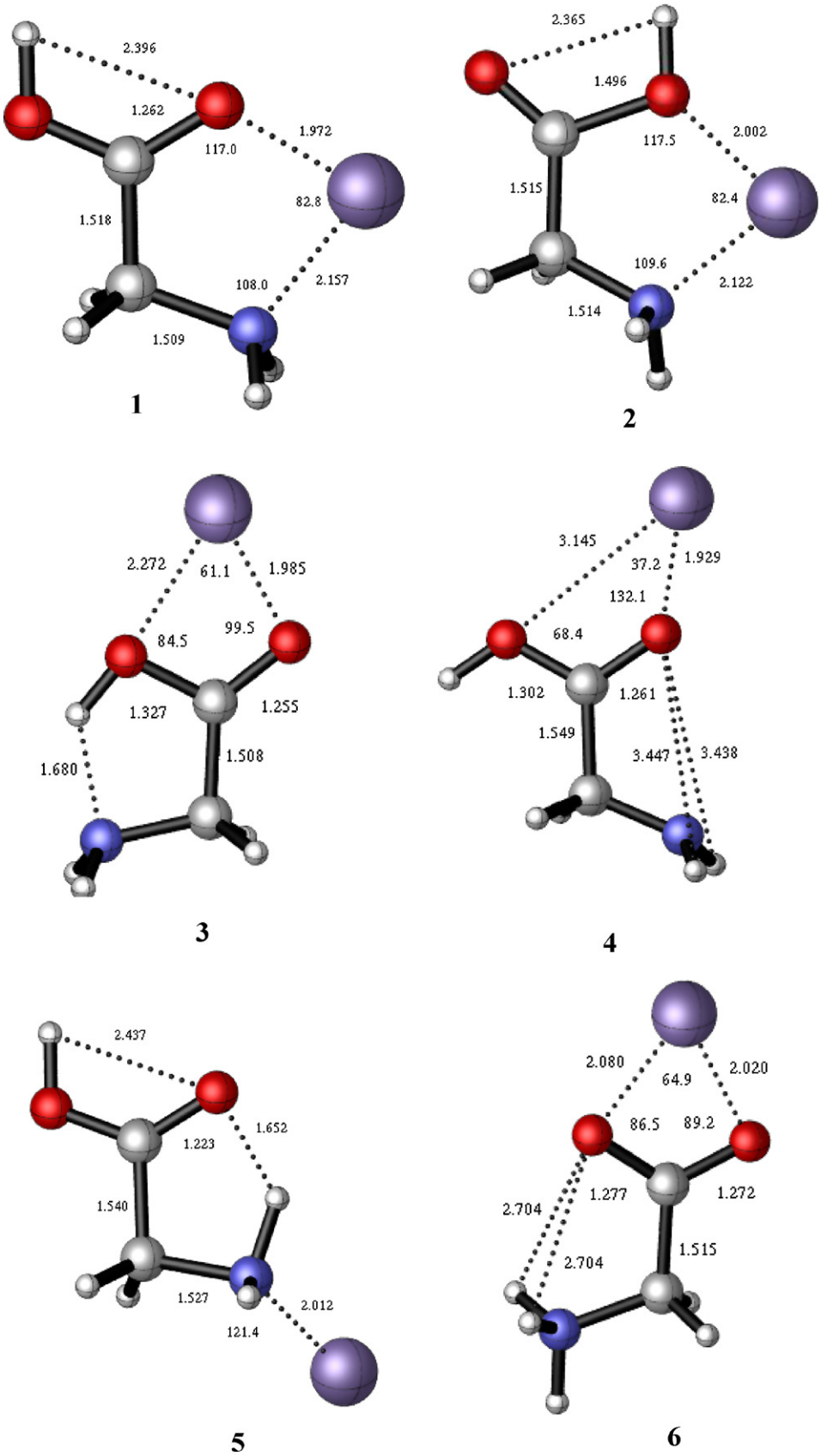


**Fig. 2.** Molecular geometry and some important structural parameters of the optimized structures for high spin ($S = 5/2$) Gly–$Mn^{2+}$ complexes at B3LYP/6-31G(d,p) level; distances and angles are given in angstrom and degree, respectively.

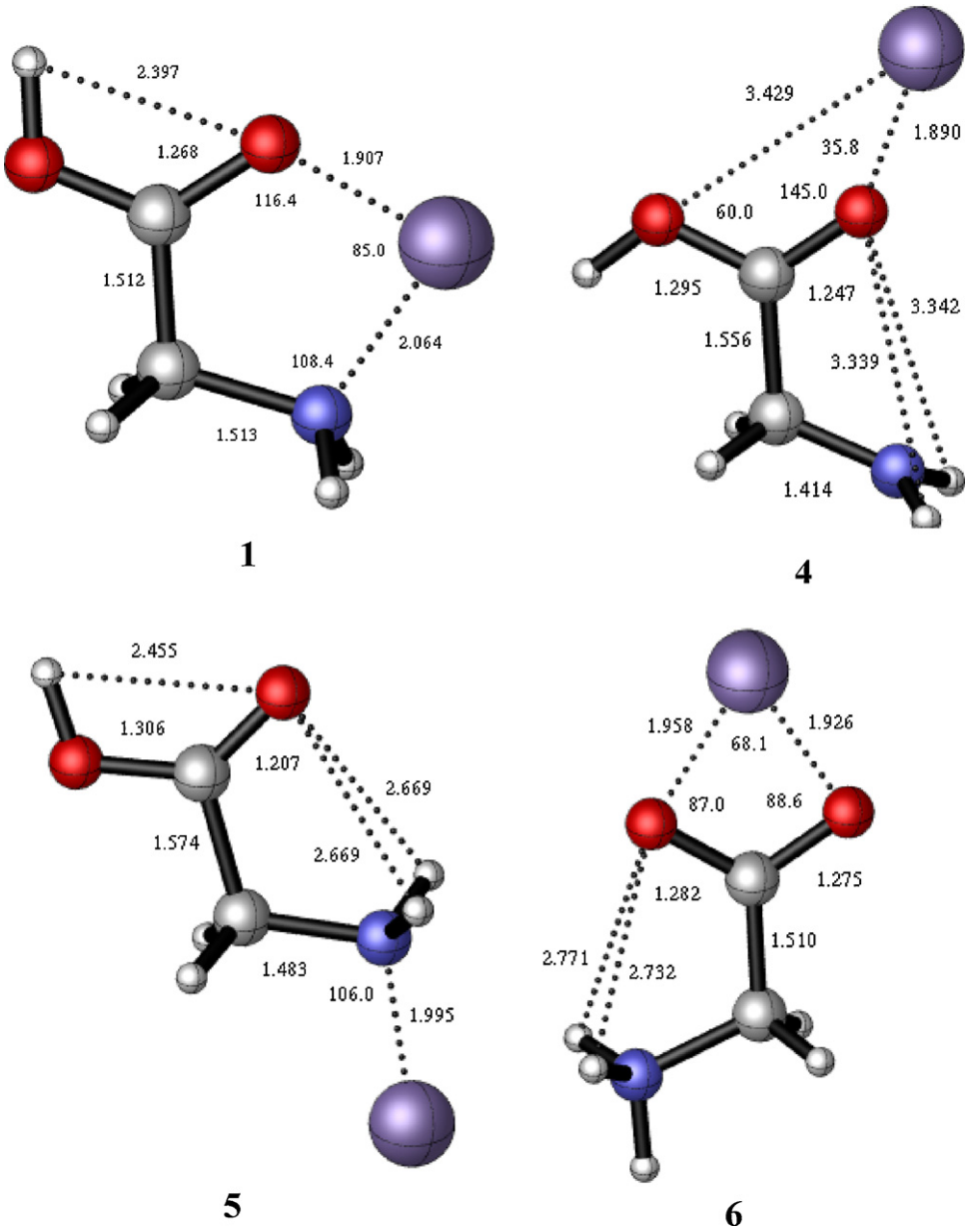


**Fig. 3.** Molecular geometry and some important structural parameters of the optimized structures for intermediate spin ($S = 3/2$) Gly–$Mn^{2+}$ complexes at B3LYP/6-31G(d,p) level; distances and angles are given in angstrom and degree, respectively.

prehensive investigations is that of Hoyau and Ohanessian [31]. Thus, in the present work, the notation proposed by the above authors has been adopted. Hence, mentioned conformations of glycine were considered for geometry optimization. Selected geometries of considered conformers are shown in Fig. 1. Although our results on glycine conformers are similar to those of some of the above studies, we have included them in the present work because we found it interesting to compare them with our computed results. As has been reported elsewhere [31,45–52], in the gas phase, glycine could be either a canonical structure in which glycine bears no formal charge or a salt bridge structure in which it is a zwitterion. It is known that glycine exists in neutral form and the **1S** conformation is the most stable with a $C_S$ symmetry [31,45–52]. The second most stable conformer is **31**. The **Z** conformer is not a minimum on the potential energy surface of glycine. Regarding our results, it is observed that the main structural features of these conformations are in complete accord with previous studies (not shown) [31,45–52]. The relative energies of these conformations have been compared with other works in Table 1. The obtained energy ordering is consistent with the energy values determined by various quantum chemical calculations at several levels [31,46–49]. The good agreement with energy ordering obtained for the different conformers of glycine further supports the reliability of both computational levels employed herein.

### 3.2. Modes of interaction between $Mn^{2+}$ and glycine

The manganese cation is an open shell system with a $3d^5$ ($^6S$) ground state [72]. Several possible electronic states are arising from the different occupations of the 3d orbitals. The starting structures of interaction between $Mn^{2+}$ and glycine involve coordination of $Mn^{2+}$ on the different electron rich sites of glycine while retaining hydrogen bonding in glycine as much as possible [31,46–49]. Our choice of starting structures for geometry optimization is analogous to that of copper complexes of glycine by Hoyau and Ohanessian [31]. The Gly–$Mn^{2+}$ complex could also be either a charge sol-

**Table 2**
Relative energies (in kcal/mol) of Gly–$Mn^{2+}$ at B3LYP/6-31G(d,p) and MP2/basis levels; $Mn^{2+}$ is in various spin states ($S$ = 5/2, 3/2, and 1/2).

| Spin | Isomers | B3LYP/6-31G(d,p) | | MP2/basis | |
|---|---|---|---|---|---|
| | | $\Delta E^a$ | $\Delta E^b$ | $\Delta E^a$ | $\Delta E^b$ |
| $S$ = 5/2 | Gly–$Mn^{2+}$ **1** | 7.1 | 7.1 | 9.5 | 9.5 |
| | Gly–$Mn^{2+}$ **2** | 30.3 | 30.3 | 30.1 | 30.1 |
| | Gly–$Mn^{2+}$ **3** | 34.9 | 34.9 | 34.8 | 34.8 |
| | Gly–$Mn^{2+}$ **4** | 48.5 | 48.5 | 49.4 | 49.4 |
| | Gly–$Mn^{2+}$ **5** | 55.4 | 55.4 | 54.0 | 54.0 |
| | Gly–$Mn^{2+}$ **6** | 0.0 | 0.0 | 0.0 | 0.0 |
| $S$ = 3/2 | Gly–$Mn^{2+}$ **1** | 4.1 | 47.6 | 6.5 | 76.9 |
| | Gly–$Mn^{2+}$ **2** | NM[c] | NM | NM | NM |
| | Gly–$Mn^{2+}$ **3** | NM | NM | NM | NM |
| | Gly–$Mn^{2+}$ **4** | 41.4 | 84.9 | 69.8 | 140.3 |
| | Gly–$Mn^{2+}$ **5** | 65.7 | 109.2 | 66.8 | 137.3 |
| | Gly–$Mn^{2+}$ **6** | 0.0 | 43.5 | 0.0 | 70.5 |
| $S$ = 1/2 | Gly–$Mn^{2+}$ **1** | 12.9 | 99.8 | 23.6 | 138.5 |
| | Gly–$Mn^{2+}$ **2** | NM | NM | NM | NM |
| | Gly–$Mn^{2+}$ **3** | NM | NM | NM | NM |
| | Gly–$Mn^{2+}$ **4** | 56.7 | 143.6 | 57.1 | 172.0 |
| | Gly–$Mn^{2+}$ **5** | NM | NM | NM | NM |
| | Gly–$Mn^{2+}$ **6** | 0.0 | 86.9 | 0.0 | 114.8 |

[a] Relative energies in the same spin state.
[b] Relative energies in all spin states.
[c] No minimum geometry could be located.

vated structure in which glycine bears no formal charge or a salt bridge structure in which glycine is a zwitterion. Thus, the coordination of manganese ion with both forms of glycine has been considered in this work. As is evident from all previous studies [13,34,35,37,39,44], the interaction of metal cations with glycine can stabilize the zwitterionic structure more strongly than its canonical isomer, in such a way that in some cases it can become the absolute minimum. In general the two structures are competitive. It has been reported that the zwitterion stabilization is larger for doubly charged cations such as $Mg^{2+}$, $Ca^{2+}$, $Zn^{2+}$, $Co^{2+}$, and $Cu^{2+}$ [13,34,35,37,39,44].

Taking into account the above discussion, seven starting structures of interaction between $Mn^{2+}$ and glycine were employed to locate stationary points on the potential energy surface. These structures fall into three types: (i) one monocoordinated structure (**5**) in which manganese is only coordinating to the nitrogen atom; (ii) five bidentate structures in which manganese is either coordinating to the nitrogen and carbonyl oxygen atoms (**1**), or coordinating to the nitrogen and hydroxyl oxygen atoms (**2**), attached to the trans carboxyl group of neutral glycine (**3** and **4**), and attached to the carboxylate group of zwitterionic glycine (**6**), and finally (iii) one structure in which manganese can interact with both oxygens and at the same time with nitrogen in a conformation such as **51**. It is notable that the latter structure is converted to **1** during the optimization.

Figs. 2–4 depict some of the low energy optimized structures for the sextet, quartet and doublet states, respectively. Among all possibilities considered, only these structures have been characterized as local minima. The spatial symmetry of all these structures is C1. Most of these structures have already been considered in previous studies on cationized glycine [13,31–44]. According to previous reports, three coordination modes maximize the metal cation–glycine interaction [13,31–44]. Note that B3LYP and MP2 optimized geometries are very similar, with Mn–O and Mn–N distances being slightly larger at the MP2 level, by 0.03–0.05 Å. Only the B3LYP structures are reported in Figs. 2–4 for clarity.

Table 2 offers the energy ordering ($\Delta E^a$ and $\Delta E^b$ values) and the nature of stationary points. By taking a look at $\Delta E^b$ values, it is clear that the most stable complexes are high spin. As shown in Fig. 2, the high spin manganese gives six stable complexes with glycine. According to $\Delta E^a$ values in Table 2, for this spin multiplicity the absolute minimum corresponds to the bicoordinated complex (**6**). In this complex, $Mn^{2+}$ interacts with the two oxygen atoms of the $CO_2^-$ terminus of zwitterionic glycine ($\eta^2$-O,O ($CO_2^-$) coordination). As has been mentioned above, the zwitterionic structure of glycine is not a minimum on the potential energy surface; however, the strong ionic interaction between $Mn^{2+}$ and negatively charged end of the zwitterion has stabilized this form. The same structure was found to be the most stable in the case of doubly charged cations such as $Co^{2+}$, $Cu^{2+}$, $Zn^{2+}$ [13,34,35,37,39,44]. As can be seen in Table 2, the second most stable structure (**1**), $\eta^2$-N,O, corresponds to $Mn^{2+}$ cation interacting with nitrogen atom and with the carbonyl oxygen, the ground electronic state being $^6$A in high spin state. This structure is almost planar and implies the formation of a five-membered ring. The optimized structure with $\eta^2$-N,O(OH), **2**, is the third stable high spin complex. The remaining structures lie higher in energy. However, the relative energy of the remaining structures varies depending on the spin state. Supplementary data contains all relevant information. Table 3 summarizes the main structural features in two low-energy complexes, **6** and **1**.

As depicted in Fig. 3, for intermediate spin complexes only four local minima were found. Energy ordering ($\Delta E^a$) for all the structures is the same as their high spin analogues. For two complexes, namely **2** and **3**, no minimum was found in the quartet spin state. The $\Delta E^a$ values in Table 2 indicate that structures **1** and **4** are more stable relative to **6** than for the similar structures in their sextet spin states. It can also be deduced that structure **5** in its quartet spin state is less stable relative to **6** than for their counterparts in the sextet spin state. Comparing the geometrical parameters of complexes in Figs. 2 and 3 shows the decrease of metal–ligand distances in intermediate spin state relative to high ones except for the Mn···OH distance in **4**. This causes more monodentate properties of glycine in intermediate spin complexes. Another obvious difference between high and intermediate spin complexes is conversion of N–H···O strong hydrogen bonding in high spin **5** to two weak hydrogen bondings in intermediate spin **5**. In addition, in high spin **5** a considerable deviation from planarity is observed for C–C–N–Mn (about 60°), while the corresponding intermediate spin structure is approximately planar for C–C–N–Mn.

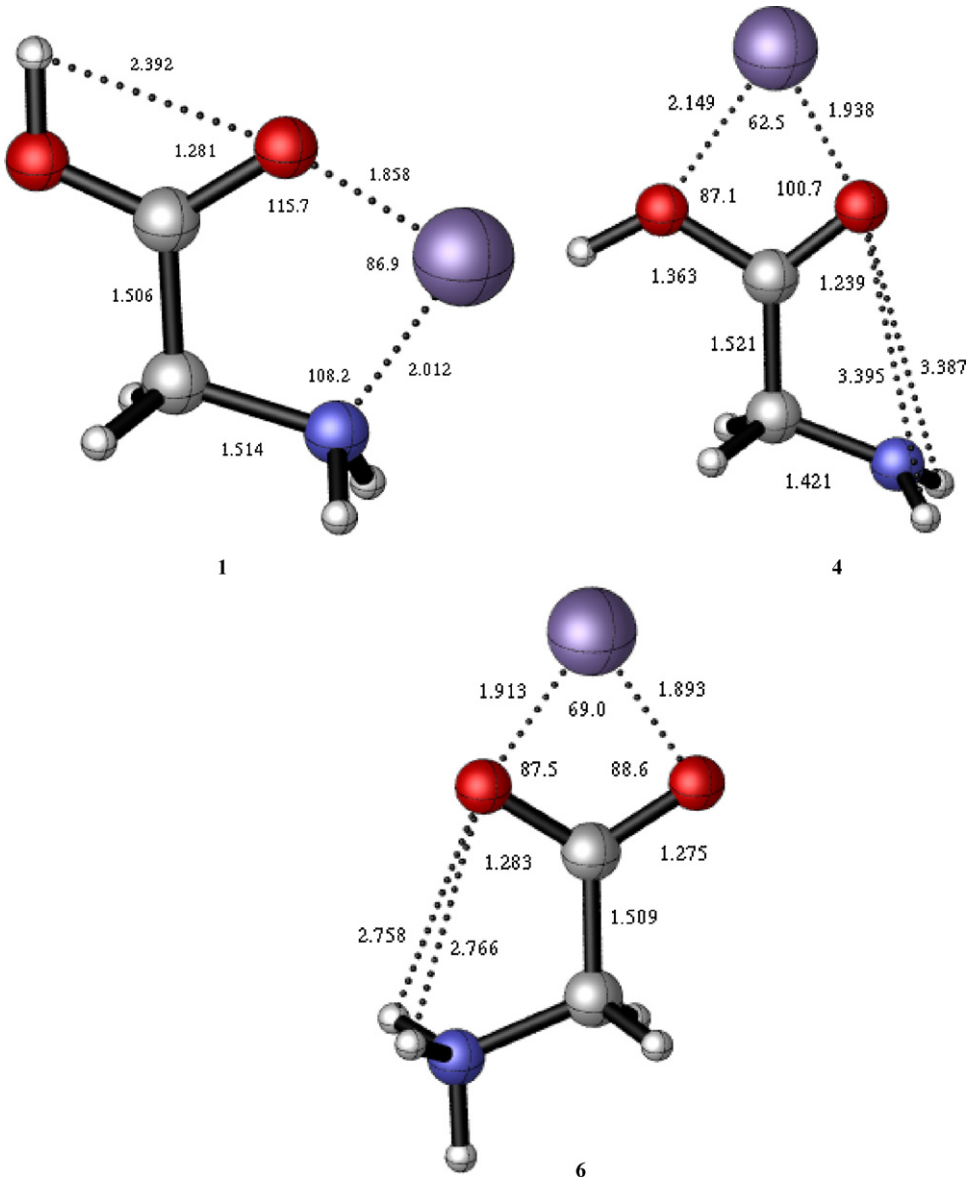


**Fig. 4.** Molecular geometry and some important structural parameters of the optimized structures for low spin ($S = 1/2$) Gly–$Mn^{2+}$ complexes at B3LYP/6-31G(d,p) level; distances and angles are given in angstrom and degree, respectively.

As shown in Fig. 4, three minima were characterized for low spin state complexes. By considering $\Delta E^a$ values for this spin state in Table 2, the same trend for energy ordering as previous spin states is observable. As can be seen in this table, there is no minimum for complex **5** along with structures **2** and **3** in the doublet spin state complexes. In contrast to what was obtained for the quartet states, structures **1** and **4** show lower stability with regard to the most stable complex, **6**, when compared with their similar sextet spin state complexes (see $\Delta E^a$ values). The unvarying shortening pattern for distances relative to higher spin state is perceived. The mentioned shortening is more sensitive in **4**. Another fact in this spin state is bidentate behavior of glycine in low spin **4** complex with respect to the two previous spin states.

While all high spin relative energies are well reproduced using B3LYP, it is less true for relative energies within intermediate or low spin isomers. Comparison of relative energies among different spin states reveals very large differences between B3LYP and MP2 results. It is not clear at this point which method is the most reliable.

### 3.3. Nature of interaction between $Mn^{2+}$ and glycine

#### 3.3.1. Molecular orbital (MO) analysis point of view

To gain some insight into the nature of binding between $Mn^{2+}$ and glycine, molecular orbital (MO) analysis has been employed. This analysis is useful to unravel the factors influencing the stability of such complexes [13,39,44]. On account of high stability of the high spin complexes relative to other complexes this section is focused mostly on the nature of binding and structures in the sextet states.

Fig. 5 shows the highest mono-occupied orbitals (HMOOs) and lowest mono-occupied orbitals (LMOOs) of high spin complexes. While the LMOOs are nearly exclusively based on Mn 3d orbitals, HMOOs include contributions of both $Mn^{2+}$ and interacting heteroatoms of glycine. All the HMOOs in this figure reveal an antibonding interaction between metal ion and ligand orbitals. These antibonding MOs are arising from the interaction of dσ orbital of the metal and lone pairs of oxygen and nitrogen atoms. All of the singly occupied molecular orbitals (SOMOs) of the most stable high spin Gly–$Mn^{2+}$ com-

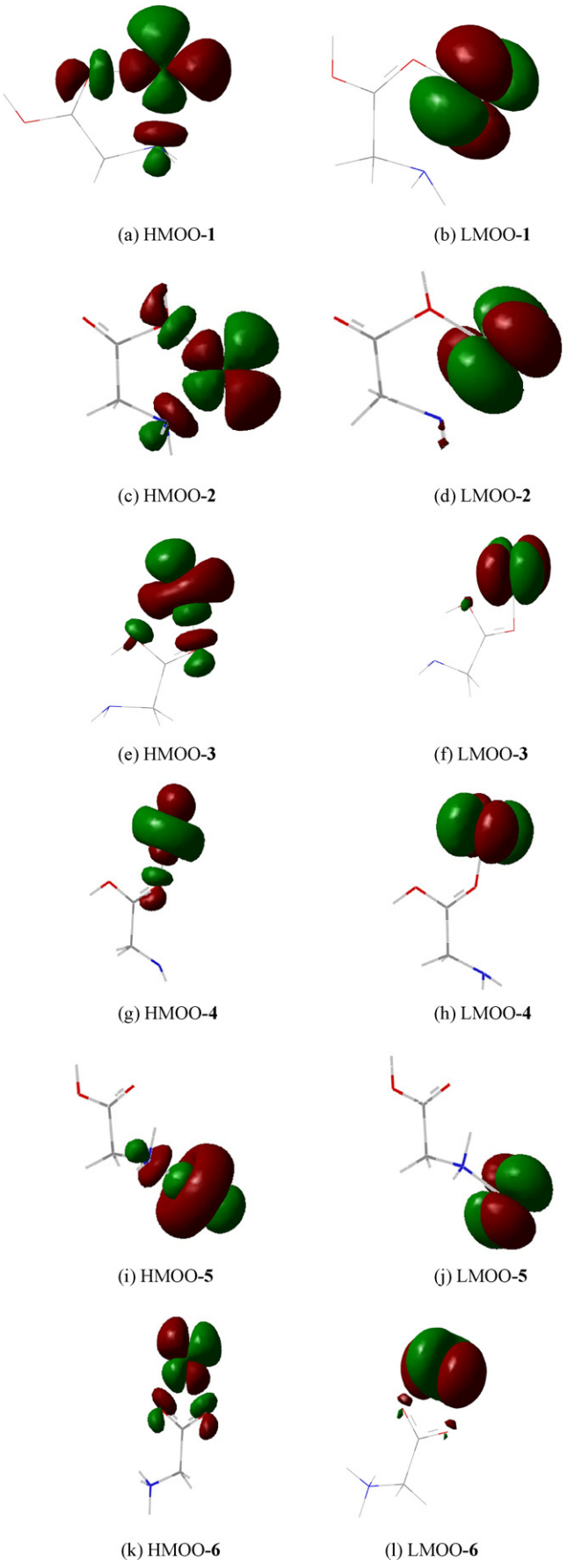


**Fig. 5.** High and low mono occupied orbitals (HMOOs and LMOOs) of different minima of high spin Gly–$Mn^{2+}$ complexes (**1**–**6**) at MP2/basis level.

**Table 3**
Selected geometrical parameters of Gly–$Mn^{2+}$ optimized structures in isomers **6** and **1** at B3LYP/6-31G(d,p) level; O1 is carbonyl oxygen except being in **6** which O1 atom is the one nearest to nitrogen.

| Isomer | Parameter | $S=5/2$ | $S=3/2$ | $S=1/2$ |
|---|---|---|---|---|
| **6** | Mn–O1 | 2.080 | 1.958 | 1.913 |
| | Mn–O2 | 2.020 | 1.926 | 1.893 |
| | Mn–O1–C | 86.5 | 87.0 | 87.5 |
| | Mn–O2–C | 89.2 | 88.6 | 88.6 |
| | O1–Mn–O2 | 64.9 | 68.0 | 69.0 |
| | C–O1 | 1.277 | 1.282 | 1.283 |
| | C–O2 | 1.272 | 1.275 | 1.275 |
| **1** | Mn–O | 1.972 | 1.907 | 1.858 |
| | Mn–N | 2.157 | 2.064 | 2.012 |
| | Mn–O–C | 117.0 | 116.4 | 115.6 |
| | O–Mn–N | 82.8 | 85.0 | 86.9 |
| | C–O | 1.281 | 1.278 | 1.273 |
| | C=O | 1.262 | 1.268 | 1.281 |
| | C–N | 1.509 | 1.513 | 1.514 |
| | O–H | 0.982 | 0.983 | 0.984 |
| | N–H | 1.026 | 1.027 | 1.027 |
| | C–O–H | 114.6 | 115.0 | 115.2 |

plex (**6**) have been included in supplementary data, Fig. I, page SD3.

In intermediate spin complexes, the manganese in quartet state interacts with the $^1A'$ state of glycine. The salt bridge isomer **6** is found to be more stable than **1** as for sextet complexes, albeit with a slightly larger difference. The HMOOs of both structures in the quartet state (Fig. 6) shows that the antibonding character is between π orbitals, leading to smaller electronic repulsion than in σ HMOOs of high spin complexes (decreasing the Pauli repulsion). This is consistent with the structural parameters listed in Table 3, which show the shortening of the Mn–O and Mn–N metal–ligand distances in intermediate spin complexes relative to high spin ones. The same trend is seen by comparing **1** and **6** in low spin complexes with their intermediate spin counterparts. One reason for this is the low contribution of ligand heteroatoms in antibonding interaction in low spin relative to intermediate spin HMOOs (see Figs. 5 and 6). The d orbitals (including doubly occupied, singly occupied, and the lowest unoccupied molecular orbitals) of the quartet state for the salt-bridge Gly–$Mn^{2+}$ complex (**6**) are presented as supplementary data, Fig. II, page SD4. A thorough analysis on the MOs arising from d orbitals of Mn in the sextet and quartet **6** complexes (Figs. I and II in supplementary data) shows that after flipping spin of one electron in the quartet state a partial electron transfer occurs in the unoccupied d orbital of the quartet complex. This fact can be evidenced by the negative energy of this MO (−0.23 eV for unoccupied d arising MO in the quartet complex versus −0.34 eV for the singly occupied MO in the sextet complex).

Taking into consideration $\Delta E^b$ values in Table 2, it is observed that at the MP2 level all high spin structures are far more stable than similar intermediate and low spin structures. For example, the least stable high spin structure (**5**) is about 16.5 and 60.8 kcal/mol more stable than the most stable complexes in intermediate and low spin states respectively. Thus, the focus will be more on high spin complexes below. Lengthening the C–N and C–O1 bond distances and approximately fixed C–C bond distance as well as maintaining the hydrogen bond in **1** relative to free Gly shows the limited deformation of Gly. Such low deformation of Gly in **1** relative to other structures corroborates with the major contribution of electrostatic and polarization interactions. This could also demonstrate the stability of **1** relative to the three remaining structures.

By taking a look at the stability of two other stable structures in Table 2, higher stability of **3** with reference to **4** in high spin states may be related to larger electrostatic interaction and maintaining N···H–O hydrogen bonding. An inversion take place in hydrogen

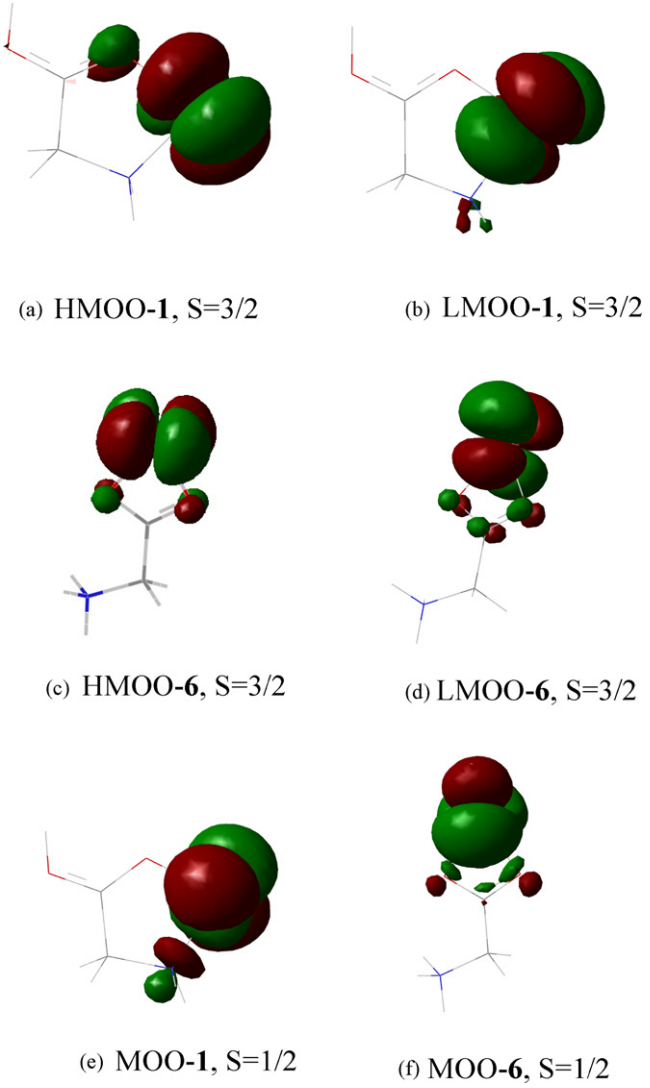


**Fig. 6.** High and low mono occupied orbitals (HMOOs and LMOOs) of the intermediate and low spin (MOOs) of **6** and **1** Gly–$Mn^{2+}$ complexes at MP2/basis level.

attached to nitrogen in **4** because of the contribution of carbonyl lone pairs in interaction to metal. As a result, the internal hydrogen bonding is diminished due to the decreasing basicity of carbonyl oxygen.

The structural parameters of Gly in lower spin complexes reveal higher deformation of these species relative to high spin ones. By paying attention to the higher relative stability of high spin **1** and **6** relative to their analogues in intermediate and low spin states, it may be concluded that the contribution of deformation energy of Gly in relative energies in various spin state is more crucial than contribution of electrostatic interaction.

**Table 5**
Relative energies (kcal/mol) of bare $Mn^{2+}$ ion and $H_2O$–$Mn^{2+}$, $NH_3$–$Mn^{2+}$, and $CH_2O$–$Mn^{2+}$ complexes in various spin states at different levels of theory.

| System | Spin | $\Delta E$ | | |
|---|---|---|---|---|
| | | B3LYP/6-31G(d,p) | MP2/basis | CCSD(T)/basis |
| $Mn^{2+}$ | $S=5/2$ | 0.0 | 0.0 | 0.0 |
| | $S=3/2$ | 75.3 | 94.0 | 95.0 |
| | $S=1/2$ | 125.3 | 205.3 | 98.4 |
| $H_2O$–$Mn^{2+}$ | $S=5/2$ | 0.0 | 0.0 | 0.0 |
| | $S=3/2$ | 68.4 | 79.7 | 76.8 |
| $NH_3$–$Mn^{2+}$ | $S=5/2$ | 0.0 | 0.0 | 0.0 |
| | $S=3/2$ | 74.5 | 80.7 | 74.5 |
| $CH_2O$–$Mn^{2+}$ | $S=5/2$ | 0.0 | 0.0 | 0.0 |
| | $S=3/2$ | 125.2 | 83.4 | 77.7 |

### 3.3.2. *Natural population analysis (NPA) point of view*

Table 4 indicates that the metal charge in all high spin complexes is larger than 1.89 and the spin density is almost entirely located on the manganese atom. This is consistent with a dominant electrostatic/polarization nature of binding. By taking into account charge and spin densities of Gly interacting sites in all structures, a strong electrostatic interaction may be also evidenced. For instance, an approximately constant charge and spin density lies on interacting oxygens in **6** which was expectable from the above discussion. The charge and spin density analyses of **1** also confirms the major contribution of electrostatics in the nature of interaction of $Mn^{2+}$ and Gly. As can be seen in Table 4, the spin density is almost focused on the manganese atom in this complex. The decreasing metal charge from sextet to quartet state complexes (by ca. 0.1e) may be associated with the existence of an empty 3d metal orbital in the latter spin state, allowing for some electron transfer from the lone pairs of Gly binding sites. The change is much smaller from the quartet to the doublet state, since the two empty orbitals can hardly be both optimally oriented for electron transfer.

## 3.4. *Complexation of $Mn^{2+}$ and small molecules*

The relative energies of the various spin states of the bare $Mn^{2+}$ ion and of $H_2O$–$Mn^{2+}$, $NH_3$–$Mn^{2+}$, and $CH_2O$–$Mn^{2+}$ complexes have been computed at different levels of theory. They are summarized in Table 5. Based on the known high energies of doublet states of bare $Mn^{2+}$ and the results described above for Gly–$Mn^{2+}$, doublet states have not been considered.

Computed interaction energies ($D_0$ and $D_e$) of complexes of $Mn^{2+}$ and some small molecules are given in Table 6. Small complexes of the type L–$Mn^{2+}$ where L is a small, non-deprotonated

**Table 4**
Natural population analysis at MP2/basis level; net atomic charges and spin density of the interacting atoms for the complexes of Gly–$Mn^{2+}$ (the spin densities are in parentheses). Total dipole moments (μ in Debye) are also included. O1 is the carbonyl oxygen except in **6** in which O1 atom is the one nearest to nitrogen.

| Spin | Isomer | State | Mn | O1 | O2 | N | μ |
|---|---|---|---|---|---|---|---|
| $S=5/2$ | Gly–$Mn^{2+}$ **1** | $^6A$ | 1.89 (4.96) | −0.93 (0.02) | – | −1.04 (0.01) | 5.67 |
| | Gly–$Mn^{2+}$ **2** | $^6A$ | 1.89 (4.96) | – | −1.01 (0.01) | −1.05 (0.01) | 8.94 |
| | Gly–$Mn^{2+}$ **3** | $^6A$ | 1.91 (4.98) | −0.88 (0.02) | −0.87 (0.00) | – | 5.01 |
| | Gly–$Mn^{2+}$ **4** | $^6A$ | 1.93 (4.98) | −0.99 (0.01) | −0.74 (0.00) | – | 8.13 |
| | Gly–$Mn^{2+}$ **5** | $^6A$ | 1.90 (4.98) | – | – | −1.17 (0.01) | 12.47 |
| | Gly–$Mn^{2+}$ **6** | $^6A$ | 1.89 (4.97) | −0.93 (0.02) | −0.91 (0.01) | – | 3.44 |
| $S=3/2$ | Gly–$Mn^{2+}$ **1** | $^4A$ | 1.80 (2.99) | −0.90 (0.01) | – | −1.01 (0.00) | 5.14 |
| | Gly–$Mn^{2+}$ **6** | $^4A$ | 1.79 (2.99) | −0.90 (0.01) | −0.86 (0.01) | – | 4.28 |
| $S=1/2$ | Gly–$Mn^{2+}$ **1** | $^2A$ | 1.79 (0.98) | −0.89 (0.00) | – | −1.03 (0.02) | 4.85 |
| | Gly–$Mn^{2+}$ **6** | $^2A$ | 1.77 (0.99) | −0.89 (0.00) | −0.86 (0.00) | – | 4.58 |

**Table 6**
Interaction energies ($D_e$, $D_0$, $\Delta H_{298}^\circ$, and $\Delta G_{298}^\circ$) of high spin $Mn^{2+}$ complexes of $NH_3$, $H_2O$, and $CH_2O$ at 298 K.

| Interaction energies | Method | $H_2O$–$Mn^{2+}$ | | $NH_3$–$Mn^{2+}$ | | $CH_2O$–$Mn^{2+}$ |
|---|---|---|---|---|---|---|
| $D_e$ | MP2 | 71.2 | 77.7[a] [76], 75.6[b] [77] | 91.9 | 95.1[b] [77] | 82.7 |
| | CCSD(T) | 74.2 | 75.7[c] [77] | 92.9 | 95.3[c] [77] | 84.4 |
| $D_0$[d] | | 72.4 | | 90.2 | | 83.1 |
| $\Delta H_{298}^\circ$[e] | | 72.0 | | 90.0 | | 82.2 |
| $\Delta G_{298}^\circ$[e] | | 77.6 | | 92.9 | | 84.4 |

[a] MP2/6-311G(d,p)//MP2/6-311G(d,p).
[b] MP2/6-311++G(d,p)//MP2/6-311++G(d,p).
[c] CCSD(T)/6-311++G(d,p)//MP2/6-311++G(d,p).
[d] Determined using CCSD(T) value and the B3LYP/6-31G(d,p) unscaled harmonic frequencies.
[e] After taking into consideration thermal corrections determined at the B3LYP/6-31G(d,p).

molecule cannot be formed directly by electrospray ionization [73]. This is why there are mass spectrometric studies on multi-ligated $Mn^{2+}$ complexes only [74–76]. Thus there is no experimental binding energy to which the present results could be compared. There have been reports of computed binding energies for $H_2O$–$Mn^{2+}$ and $NH_3$–$Mn^{2+}$ [76,77]. Results of our calculations in Table 6 show a good agreement with these reports. As can be seen in this table, the complex between $Mn^{2+}$ and $H_2O$ indicates a weaker interaction compared with other small molecules, in agreement with recent work [76]. As has been mentioned elsewhere [75], the relatively weak interaction of $Mn^{2+}$ and the OH end of Gly is stronger than that of $Mn^{2+}$ and $H_2O$. By taking a look at interaction energies it is revealed that the strength of small molecules complexation with $Mn^{2+}$ is in the order $H_2O < CH_2O < NH_3$. Thus manganese ion reveals higher affinity towards ammonia than the simplest carbonyl group. Accordingly, by considering the results of Blades et al. [75], it is expected that addition of other ligands, chelation, or substitution of alkyl (R) group instead of H carbonyl group (like –OH and $–CH_2–NH_2$ in Gly) increases the complexation strength and as a result makes manganese ion more stabilized.

### 3.5. Interaction energies of Gly–$Mn^{2+}$ complex

Computed interaction energies ($D_0$ and $D_e$) of **6** Gly–$Mn^{2+}$ complex are given in Table 7. As shown in this table, the B3LYP $D_e$ value is larger than its CCSD(T) counterpart by 19.2 kcal/mol (177.6 compared to 158.4 kcal/mol). It has been reported previously that B3LYP method overestimates metal ion–molecule interaction energies because of the self-interaction problem in DFT [44]. To the best of our knowledge there is no experimental data on the interaction energies of Gly–$Mn^{2+}$ complex. On the other hand, it has been emphasized that doubly charged complexes are difficult to generate due to the charge transfer dissociation processes and proton transfer reactions [44]. Thus, the present computations of interaction energies for the Gly–$Mn^{2+}$ complex provide new insight into the strong binding of manganese.

**Table 7**
Interaction energies ($D_e$, $D_0$, $\Delta H_{298}^\circ$, and $\Delta G_{298}^\circ$) of high spin ($S = 5/2$) Gly–$Mn^{2+}$ complex **6** (in kcal/mol).

| Interaction energies | Method | $Mn^{2+}$, $^6A$ |
|---|---|---|
| $D_e$ | B3LYP | 177.6 |
| | MP2 | 156.4 |
| | CCSD(T) | 158.4 |
| $D_0$[a] | | 156.1 |
| $\Delta H_{298}^\circ$[b] | | 155.3 |
| $\Delta G_{298}^\circ$[b] | | 159.3 |

[a] Determined using CCSD(T)/basis values and the B3LYP/6-31G(d,p) unscaled harmonic frequencies.
[b] After taking into consideration thermal corrections determined at the B3LYP/6-31G(d,p).

### 3.6. Vibrational spectrum of Gly–$Mn^{2+}$ complexes

There has been considerable recent interest in the structural information that infrared spectroscopy can yield on metal ion complexes of amino acids [53]. In this context, the computed IR spectra of Gly–$Mn^{2+}$ complexes are valuable in predicting the experimental vibrational spectra since the complexation of $Mn^{2+}$ with glycine has not been investigated so far. The IR spectra of the most stable structures of high spin Gly–$Mn^{2+}$ complexes (**1** and **6**) computed at the B3LYP/6-31G(d,p) level are displayed in Fig. 7(a) and (b), respectively.

The main features in the spectrum of **1** include a dominant C=O stretch component at 1628 $cm^{-1}$ and a less intense $NH_2$ scissor band at 1611 $cm^{-1}$. While neither mode exists in **6**, there are two less intense bands in the same frequency range in the spectrum of **6**, at 1608 and 1612 $cm^{-1}$. Both are scissoring modes of the ammonium group. Thus this region cannot lead to clear distinc-

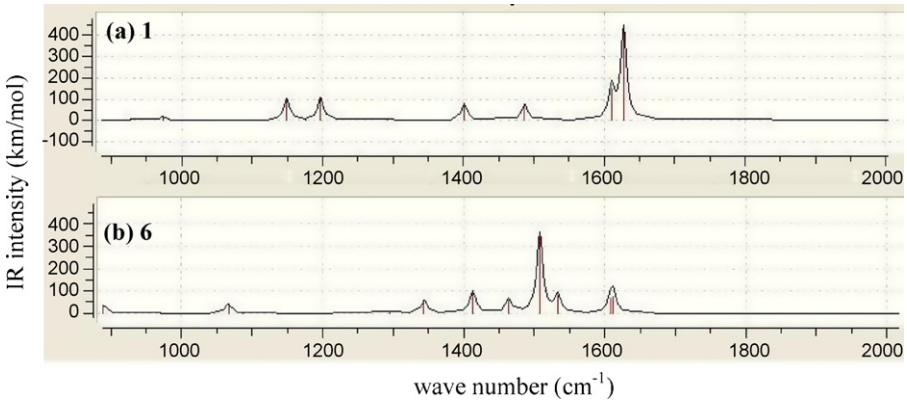


**Fig. 7.** Computed spectra of the most thermodynamically favored high spin Gly–$Mn^{2+}$ complexes at the B3LYP/6-31G(d,p) level. The frequencies have been scaled by 0.97.

tion between **1** and **6**. The carboxylate stretches could in principle be helpful (at 1508 and 1464 $cm^{-1}$, respectively), however their low intensities make their identification difficult. The most specific and intense signature is that of the ammonium umbrella motion at 1508 $cm^{-1}$ in the spectrum of **6**, which is intense and in a relatively silent part of the spectrum of **1**. Conversely, the COH bending motion, which leads to a band at 1149 $cm^{-1}$ in the spectrum of **1**, is absent from that in **6**. Although less intense, it may also serve as a structural identification tool.

IRMPD spectra of amino acids attached to divalent metal ions have been published recently [78–81]. It was found that several diagnostic bands are red shifted in doubly charged complexes relative to their positions in singly charged complexes. The present results confirm this trend. A recent report on the IRMPD spectra of two tryptophan molecules attached to several divalent metal ions including $Mn^{2+}$ revealed that in most cases, including $Mn^{2+}Trp_2$, the observed structure involves one CS and one SB complexation mode. In this respect, manganese was found to be rather similar to other metal dication including $Co^{2+}$ and $Zn^{2+}$, while $Ni^{2+}$ was found to behave differently [81]. The $Ba^{2+}$Trp complex was the first for which an IRMPD spectrum was obtained for a doubly charged metal ion and a singly amino acid attached [78]. The intense peak near 1450 $cm^{-1}$ arising from the $NH_3^+$ umbrella motion is in good agreement with the computed peak displayed for **6** in Fig. 7(b).

## 4. Conclusions

Quantum chemical calculations have been performed in order to identify the $Mn^{2+}$ binding sites of glycine. Seven modes of Gly–$Mn^{2+}$ interaction were considered as starting structures in each case. Stable complexes on the potential energy surface have been located. It has been found that among three possible spin state of $Mn^{2+}$ including high, low, and intermediate spins in Gly–$Mn^{2+}$ complex, the most stable complex is high spin. Two low energy complexes were characterized in each spin state: one in which the metal ion interacts with the carboxylate terminus of zwitterionic glycine ($\eta^2$-O,O ($CO_2^-$)), and another in which it chelates with the amino nitrogen and the carbonyl oxygen of neutral glycine ($\eta^2$-O,N). Analysis of the nature of metal–glycine binding shows that the large electrostatic interaction established with the zwitterionic conformation of glycine makes the bidentate coordination with carboxylate group the most stable structure. The gas phase interaction energy of manganese cation ($Mn^{2+}$) with glycine (**6**) was established at B3LYP, MP2 and CCSD(T) levels of theory. Finally, the computed IR spectra of the most stable structures of the high spin Gly–$Mn^{2+}$ complexes were discussed.

## Supplementary data

Optimized structures and total energies as well as zero point corrections of all considered complexes and the conformers of glycine.

## Acknowledgement

The financial support of Research Council of Shahid Beheshti University is gratefully acknowledged.

## Appendix A. Supplementary data

Supplementary data associated with this article can be found, in the online version, at doi:10.1016/j.ijms.2010.01.012.

## References

[1] I. Bertini, H.B. Gray, S.J. Lippard, Bioinorganic Chemistry, University Science Books, California, 1994.
[2] G.C. Dismukes, Chem. Rev. 96 (1996) 2909.
[3] C.L. Schram, F.C. Wedler, Manganese in Metabolism and Enzyme Function, Academic, New York, 1986.
[4] D. Wöhrle, A.D. Pomogaĭlo, Metal Complexes and Metals in Macromolecules: Synthesis, Structure and Properties, Wiley-VCH, 2003.
[5] L.P. Vincent, M.J. Baldwin, A. Gelasco, Chem. Rev. 94 (1994) 807.
[6] N. Niccolai, E. Tiezzi, G. Valensin, Chem. Rev. 82 (1982) 359.
[7] L.M. Weiner, J.M. Backer, Rezvukhin, A.I. Biochim, Biophys. Acta 383 (3) (1975) 316.
[8] F.W. McLafferty, H.D.R. Schuddenmage, J. Am. Chem. Soc. 62 (1969) 1866.
[9] R.G. Cooks, Collision Spectroscopy, Plenum Press, New York, 1978.
[10] M.W. Senko, J.P. Speir, F.W. McLafferty, Anal. Chem. 66 (1994) 1866.
[11] J.P. Glusker, Adv. Protein Chem. 42 (1991) 1.
[12] E.T. Adman, Adv. Protein Chem. 42 (1991) 144.
[13] J. Bertran, L. Rodriguez-Santiago, M. Sodupe, J. Phys. Chem. B 103 (1999) 2310.
[14] R.P. Grese, R.L. Cerny, M.L. Gross, J. Am. Chem. Soc. 111 (1989) 2835.
[15] P. Hu, M.L. Gross, J. Am. Chem. Soc. 114 (1992) 9153.
[16] P. Hu, M.L. Gross, J. Am. Chem. Soc. 115 (1993) 8821.
[17] L.M. Teesch, J. Adams, J. Am. Chem. Soc. 112 (1990) 4110.
[18] L.M. Teesch, J. Adams, J. Am. Chem. Soc. 113 (1991) 812.
[19] A. Reiter, J. Adams, H. Zhao, J. Am. Chem. Soc. 116 (1994) 7827.
[20] Q.P. Lei, I.J. Amster, J. Am. Soc. Mass Spectrom. 7 (1996) 722.
[21] V.W.M. Lee, H. Li, T.C. Lau, R. Guevremont, K.W.M. Siu, J. Am. Soc. Mass Spectrom. 9 (1998) 760.
[22] B.A. Cerda, C. Wesdemiotis, Int. J. Mass Spectrom. 185/186/187 (1999) 107.
[23] H. Lavanant, E. Hecquet, Y. Hoppilliard, Int. J. Mass Spectrom. 185/186/187 (1999) 11.
[24] T. Wyttenbach, M. Witt, M.T. Bowers, J. Am. Chem. Soc. 122 (2000) 3458.
[25] F. Rogalewicz, Y. Hoppilliard, G. Ohanessian, Int. J. Mass Spectrom. 201 (2000) 307.
[26] Y. Hoppilliard, F. Rogalewicz, G. Ohanessian, Int. J. Mass Spectrom. 204 (2000) 267.
[27] F. Rogalewicz, Y. Hoppilliard, G. Ohanessian, Int. J. Mass Spectrom. 206 (2001) 45.
[28] R.M. Moision, P.B. Armentrout, J. Phys. Chem. A 106 (2002) 10350.
[29] F. Rogalewicz, Y. Hoppilliard, G. Ohanessian, Int. J. Mass Spectrom. 227 (2003) 439.
[30] M.M. Kish, G. Ohanessian, C. Wesdemiotis, Int. J. Mass Spectrom. 227 (2003) 509.
[31] S. Hoyau, G. Ohanessian, J. Am. Chem. Soc. 119 (1997) 2016.
[32] S. Hoyau, G. Ohanessian, Chem. Eur. J. 4 (1998) 1561.
[33] T. Marino, N. Russo, N. Toscano, J. Inorg. Biochem. 79 (2000) 179.
[34] F. Rogalewicz, G. Ohanessian, N. Gresh, J. Comput. Chem. 21 (2000) 963.
[35] E.F. Strittmatter, A.S. Lemoff, E.R. Williams, J. Phys. Chem. A 104 (2000) 9793.
[36] S. Pulkkinen, M. Noguera, L. Rodriguez-Santiago, M. Sodupe, J. Bertran, Chem. Eur. J. 6 (2000) 4393.
[37] S. Hoyau, J.P. Pelicier, F. Rogalewicz, Y. Hoppilliard, G. Ohanessian, Eur. J. Mass Spectrom. 7 (2001) 303.
[38] M.M. Kish, C. Wesdemiotis, G. Ohanessian, J. Phys. Chem. B 108 (2004) 3086.
[39] L. Rodrıguez-Santiago, M. Sodupe, J. Tortajada, J. Phys. Chem. A 105 (2001) 5340.
[40] T. Shoeib, C.F. Rodrıguez, K.W.M. Siu, A.C. Hopkinson, Phys. Chem. Chem. Phys. 3 (2001) 853.
[41] T. Shoeib, K.W.M. Siu, A.C. Hopkinson, J. Phys. Chem. A 106 (2002) 6121.
[42] C.H.S. Wong, F.M. Siu, N.L. Ma, C.W. Tsang, J. Mol. Struct. (Theochem.) 588 (2002) 9.
[43] C. Kapota, J. Lemaire, P. Maitre, G. Ohanessian, J. Am. Chem. Soc. 126 (2004) 1836.
[44] E. Constantino, L. Rodriguez-Santiago, M. Sodupe, J. Tortajada, J. Phys. Chem. A 109 (1) (2005) 224.
[45] J.H. Jensen, M.S. Gordon, J. Am. Chem. Soc. 117 (1995) 8159.
[46] F. Jensen, J. Am. Chem. Soc. 114 (1992) 9533.
[47] C.H. Hu, M. Shen, H.F. Schaefer, J. Am. Chem. Soc. 115 (1993) 2923.
[48] A.G. Czaszar, J. Am. Chem. Soc. 114 (1992) 9568.
[49] V. Barone, C. Adamo, F. Lejl, J. Chem. Phys. 102 (1995) 364.
[50] F. Lejl, C. Adamo, V. Barone, Chem. Phys. Lett. 230 (1994) 189.
[51] S.G. Stepanian, I.D. Reva, E.D. Radchenko, M.T.S. Rosado, M.L.T.S. Duarte, R. Fausto, L. Adamowicz, J. Phys. Chem. A 102 (1998) 1041.
[52] S.G. Stepanian, I.D. Reva, E.D. Radchenko, L. Adamowicz, J. Phys. Chem. A 102 (1998) 4623.
[53] N.C. Polfer, J. Oomens, Mass Spectrom. Rev. 28 (2009) 468.
[54] R. Kaschner, D. Hohl, J. Phys. Chem. A 102 (1998) 5111.
[55] S. Sirois, E.I. Proynov, D.T. Nguyen, D.R. Salahub, J. Chem. Phys. 107 (1997) 6770.
[56] A.D. Becke, J. Chem. Phys. 98 (1993) 5648.
[57] A.D. Becke, Phys. Rev. A 38 (1988) 3098.
[58] C. Lee, W. Yang, R.G. Parr, Phys. Rev. B 37 (1988) 785.
[59] C. Møller, M.S. Plesset, Phys. Rev. 46 (1934) 618.
[60] J.A. Pople, R. Krishnan, H.B. Schlegel, J.S. Binkley, Int. J. Quantum Chem. Symp. 13 (1979) 325.
[61] M.C. Holthausen, M. Mohr, W. Koch, Chem. Phys. Lett. M 240 (1995) 245.
[62] M.R.A. Blomberg, P.E.M. Siegbahn, M. Svensson, J. Chem. Phys. 104 (1996) 9546.
[63] C.W. Bauschlicher, A. Ricca, H. Partridge, S.R. Langhoff, Recent Advances in Density Functional Theory, Part II, World Scientific Publishing Co., Singapore, 1997.
[64] A. Luna, M. Alcami, O. Mo, M. Yanez, Chem. Phys. Lett. 320 (2000) 129.
[65] W. Koch, M.C. Holthausen (Eds.), A Chemist's Guide to Density Functional Theory, 2nd ed., Wiley-VCH Verlag, Weinheim, Germany, 2001.

[66] E.R. Davidson, D. Feller, Chem. Rev. 86 (4) (1986) 681.
[67] W.J. Hehre, L. Radom, P.V. Schleyer, J. Pople, Ab initio Molecular Orbital Theory, Wiley, New York, 1998.
[68] A.J.H. Wachters, J. Chem. Phys. 52 (1970) 1033.
[69] K. Raghavachari, G.W. Trucks, J.A. Pople, M. Head-Gordon, Chem. Phys. Lett. 157 (1989) 479.
[70] F. Weinhold, J.E. Carpenter, The Structure of Small Molecules and Ions, Plenum, New York, 1988.
[71] M.J. Frisch, G.W. Trucks, H.B. Schlegel, G.E. Scuseria, M.A. Robb, J.R. Cheeseman, V.G. Zakrzewski, J.A. Montgomery, R.E. Stratmann, J.C. Burant, S. Dapprich, J.M. Millam, A.D. Daniels, K.N. Kudin, M.C. Strain, O. Farkas, J. Tomasi, V. Barone, M. Cossi, R. Cammi, B. Mennucci, C. Pomelli, C. Adamo, S. Clifford, J. Ochterski, G.A. Petersson, P.Y. Ayala, Q. Cui, K. Morokuma, D.K. Malick, A.D. Rabuck, K. Raghavachari, J.B. Foresman, J. Cioslowski, J.V. Ortiz, B.B. Stefanov, G. Liu, A. Liashenko, P. Piskorz, I. Komaromi, R. Gomperts, R.L. Martin, D.J. Fox, T. Keith, M.A. Al-Laham, C.Y. Peng, A. Nanayakkara, C. Gonzalez, M. Challacombe, P.M.W. Gill, B.G. Johnson, W. Chen, M.W. Wong, J.L. Andres, M.R.E.S. Head-Gordon, J.A. Pople, Gaussian 98, Gaussian, Inc., Pittsburg, PA, 1998.
[72] H. Avelino de Abreu, L. Guimaraes, H.A. Duarte, Int. J. Quantum Chem. 108 (2008) 2467.
[73] A.T. Blades, P. Jayaweera, M.G. Ikonomou, P. Kebarle, J. Chem. Phys. 92 (1990) 5900.
[74] U.N. Andersen, G. Bojesen, Int. J. Mass Spectrom. 153 (1996) 1.
[75] A.T. Blades, P. Kebarle, J. Phys. Chem. A 110 (2006) 12055.
[76] B.J. Duncombe, J.O.S. Ryden, L. Puskar, H. Cox, A.J. Stace, J. Am. Soc. Mass Spectrom. 19 (2008) 520.
[77] M. Trachtman, C.W. Bock, J. Mol. Struct. (Theochem.) 672 (2004) 75.
[78] R.C. Dunbar, N.C. Polfer, J. Oomens, J. Am. Chem. Soc. 129 (2007) 14562.
[79] M.F. Bush, J. Oomens, R.J. Saykally, E.R. Williams, J. Am. Chem. Soc. 130 (2008) 6463.
[80] J.T. O'Brien, J.S. Prell, J.D. Steill, J. Oomens, E.R. Williams, J. Phys. Chem. A 112 (2008) 10823.
[81] R.C. Dunbar, J.D. Steill, N.C. Polfer, J. Oomens, J. Phys. Chem. A 113 (2009) 845.